J Mol Model (2014) 20:2490
DOI 10.1007/s00894-014-2490-3

ORIGINAL PAPER

# Chemisorption-induced two- to three-dimensions structural transformations in gold pentamer $(CO)_nAu_5^-$ (n =0–5)

**Ming-Min Zhong · Xiao-Yu Kuang · Zhen-Hua Wang · Hong-kuan Yuan · Hong Chen**

Received: 8 May 2014 / Accepted: 6 October 2014 / Published online: 24 October 2014


**Abstract** Understanding the geometry structures of gold clusters, especially with adsorbates, is essential for designing highly active gold nanocatalysts. Here, CO chemisorption onto the $Au_5^-$ cluster is investigated using the density functional calculations. It is found that chemisorption of CO molecules can induce previously unreported two- to three-dimensions (3D) structural changes. Even a single CO chemisorption induces a major structural change to explain the huge blue-shift in photoelectron spectroscopy (PES). The apex site in the parent $Au_5^-$ cluster is not always the most preferred site for the chemisorption, and two bridged adsorption CO molecules are observed in the lowest-energy $(CO)_3Au_5^-$ cluster. A clear splitting is observed in the first PES of $(CO)_4Au_5^-$, and calculated planar and 3D geometries are likely coexisting in the cluster beam. The fifth CO adsorption leads to the structural transformation of $Au_5$ skeleton to create more apex sites to accommodate five CO molecules. The structural properties, together with the vertical electron detachment energy (VDE) and binding energies calculations indicate that the chemisorption-saturated number is 5.

**Keywords** Chemisorption · Gold pentamer carbonyl complex · IR spectrum · 2D to 3D structural transformation

**Electronic supplementary material** The online version of this article (doi:10.1007/s00894-014-2490-3) contains supplementary material, which is available to authorized users.

M.-M. Zhong (✉) · H.-k. Yuan · H. Chen
School of Physical Science and Technology, Southwest University, Chongqing 400715, China
e-mail: scu_zmm@163.com

X.-Y. Kuang · Z.-H. Wang
Institute of Atomic and Molecular Physics, Sichuan University, Chengdu 610065, China

## Introduction

Since the discovery of remarkable catalytic activities of highly dispersed gold nanoparticles for low-temperature CO oxidation [1–3], a growing list of important reactions have been found to be catalyzed by gold nanoparticles, such as expoxidation [4, 5], hydrogenation [6], C-C bond formation [7], and water-gas shift [8]. A number of such studies have been devoted to the reactivity and chemisorption properties of CO oxidation [9]. Many factors have been reported to influence the rate of CO oxidation, including cluster size, shape, and oxidation/charge state, as well as support and methods for preparation of gold nanoparticles. Numerous models have been proposed, including the perimeter sites model [1, 2], the nonmetallic gold model [10], the extra electron model [11, 12], the two atomic layers model [13], and the low-coordination sites model [14, 15]. However, the exact catalytic mechanisms for CO oxidation are still under debate. Recent experimental and theoretical studies have been established that CO or $O_2$ adsorbs molecularly on the well-defined gold clusters and nanoparticles [16–18]. Coadsorption of CO or $O_2$ on small gold clusters has been investigated by mass-spectrometry-based experiments and by DFT calculations [19–21]. Importantly, it is revealed that CO and $O_2$ adsorb cooperatively rather than competitively. Small-sized charge and neutral gold clusters show CO binding ability. In addition, corner or apex atoms have been found to be the preferred site for the CO binding.

The gold clusters are usually firm after a single CO molecule adsorption without major structural transformation, upon the multiple COs adsorption, the significant structural changes have been observed [16, 17, 22–24]. The photoelectron spectroscopy (PES) of several series of gold carbonyl clusters anions $(CO)_nAu_m^-$ ($n$ =1–7, $m$ =2–5) have been reported by Zhai et al. [25]. For each gold cluster, CO adsorption reaches a critical number, beyond which further CO adsorption hardly

changes the spectra. The critical CO number corresponds exactly to the available low-coordinate apex sites in the corresponding bare Au clusters. Using photoelectron spectroscopy (PES) and ab initio calculations, it is found that the gold heptamer $Au_7^-$ is an unusually flexible cluster and CO binding can induce unreported 2D–3D–2D structural changes [26]. As to $Au_6^-$, it can maintain its triangular structure when it binds up to three molecules [22]. While starting from the adsorption of the fourth CO, significant structural change occurs at $Au_6^-$ to chemosorb up to six COs [27]. Chemisorption of CO molecule exerts great influence on the geometry structures of anion gold hexamer and heptamer. However, the information on the geometry structures of anion gold pentamer framework upon CO adsorption is still scare. The questions thus arise: where do the multiple CO molecules bind to the anion gold pentamer, what is the chemisorption saturation limit of CO, and how does the structure change after the multi-CO adsorption. The goal of the current work is to answer these questions. Answers to these questions may provide further insight into the nature of CO interactions with Au clusters and understanding of the cooperative chemisorption of CO and $O_2$ during the catalytic formation of $CO_2$.

In the current article, we report a systemically theoretical study on a series of gold carbonyl clusters: $(CO)_nAu_5^-$ ($n$ =0–5). The geometry properties, structure transformation, chemisorption and physisorption regime, IR spectra, and binding energies of the gold pentamer upon multi-CO adsorption are investigated. Even with chemisorption of a single CO, a major structural change occurs at $Au_5^-$. The unusual bridged site adsorption is observed in the $(CO)_3Au_5^-$ cluster. Chemisorption of CO molecules can induce previously unreported two- to three-dimensions (3D) structure changes. This CO adsorption induced structural change in gold pentamer is interesting and analogous to structural flexibility and mobility in heterogeneous catalysis. The observations of CO adsorption site and CO-induced structural change in small gold clusters may be important for understanding the mechanisms of CO oxidation on supported gold nanoparticles.

## Computational details

We employed the Stuttgart/Dresden double-zeta SDD basis set for gold [28, 29], and the standard all-electron basis set 6-311+G(3df) for oxygen and carbon. A variety of exchange-correlation (XC) functionals including the generalized gradient approximation (GGA: PBE) [30], hybrid GGA (B3LYP) [31], and meta-GGA (TPSS) [32] were used to investigate the accuracies of DFT methods on the geometries and energies of $(CO)_nAu_5^-$. Results were summarized in Table 1. It can be noted that the results are quite sensitive to the choice of the exchange-correlation functionals. As many low-lying structures of $(CO)_nAu_5^-$ ($n$ =0–5) are almost degenerate in energy at the DFT level. All calculations were carried out with the GAUSSIAN 03 program [33].

The total energies of these clusters were then applied to study the evolution of their relative stability, CO adsorption energy, and vertical electron detachment energy (VDE). Because the computed zero-point energy (ZPE) corrections of the isomers of a specific cluster size were small and almost the same, they were not expected to affect the relative energy ordering. All charge populations were obtained with the natural population analysis (NPA). Vertical electron detachment energies (VDEs) were obtained at the anion geometry by using a combined ΔSCF-DFT approach [23], where the first VDE was calculated from the difference between the ground-state energies of anions and neutrals (i.e., ΔSCF) and the higher VDEs were calculated from the ground-state energy of the anions and excited-state energies of neutrals by using TD-DFT. Three criteria were used in comparing the theoretical results with the experimental data to select our most likely candidate structures: 1) relative energies, 2) the first VDE, and 3) higher VDEs. Only those isomers that meet three criteria were considered to be the superlative candidates for $(CO)_nAu_5^-$ ($n$ =0–5) clusters.

## Results and discussion

### Geometries of $Au_5^-$ anion

To date, a great effort has been made to elucidate the geometry structures of gold clusters. Detailed structure information on small anionic gold clusters has been obtained by photoelectron spectroscopy combined with DFT calculations [34, 35]. The gold anion clusters are reported to have planar structures at n =3–12, and 3D structures at n ≥12. In this work, we focus on the gold pentamer. Our calculations for some low-lying structures of gold pentamer with various functionals (Table 1) indicate that the V-shaped isomer 0-a is lower than the well-known trapezoidal structure 0-b (Fig. 1). The isomer 0-a is lower than the trapezoidal one in energy by 0.08 eV (PBE), 0.04 eV (TPSS), and 0.27 eV (B3LYP), respectively. The DFT energy difference of two isomers is negligible and these two isomers are almost degenerate. In order to confirm the optimal isomer, we further calculate the VDE of the anion gold pentamer. It is found that the VDEs of isomers 0-a and 0-b are 4.08 and 3.14 eV at PBE level, respectively. The similar results are found at the other XC functionals. All calculated results indicate that the VDE of the trapezoidal isomer is consistent with the experimental data (3.11 eV) [25]. The isomer 0-a of $Au_5^-$ is quite different from the most stable structure of neutral and cation $Au_5$ clusters, in which the trapezoidal one is preferred, indicating the dependence of geometry structure on the charge state of gold cluster.

**Table 1** Geometries, symmetries, electron state, relative energies RE (eV), and vertical electron detachment energies VDE (eV) compared with the experimental data for the $(CO)_nAu_5^-$ (n =0–5) clusters at different level

| Geo. | | PBE | | | | TPSS | | B3LYP | | Exp.[25] |
|---|---|---|---|---|---|---|---|---|---|---|
| | | Sym. | State | RE | VDE | RE | VDE | RE | VDE | VDE |
| $Au_5^-$ | 0-a | $C_{2v}$ | $1A_1$ | 0.00 | 4.08 | 0.00 | 3.96 | 0.00 | 4.09 | |
| | 0-b | $C_{2v}$ | $1A_1$ | 0.08 | 3.14 | 0.04 | 2.99 | 0.27 | 3.14 | 3.11(3) |
| | 0-c | $C_{2v}$ | $1A_1$ | 0.21 | 3.65 | 0.19 | 2.51 | 0.30 | 3.72 | |
| | 0-d | $D_{2h}$ | $1A_g$ | 0.73 | 2.96 | | | 0.91 | 2.91 | |
| | 0-e | $C_{4v}$ | $1A_1$ | 1.03 | 3.24 | 0.96 | 3.05 | | | |
| $(CO)Au_5^-$ | 1-a | $C_{2v}$ | $1A_1$ | 0.00 | 3.73 | 0.00 | 3.63 | 0.00 | 3.67 | 4.02(3) |
| | 1-b | $C_s$ | $1A'$ | 0.27 | 3.81 | 0.28 | 3.72 | 0.21 | 3.84 | |
| | 1-c | $C_s$ | $1A'$ | 0.31 | 3.37 | 0.28 | 2.96 | 0.45 | 3.06 | |
| | 1-d | $C_{2v}$ | $1A'$ | 0.33 | 4.08 | 0.31 | 3.53 | 0.33 | 3.78 | |
| | 1-e | $C_s$ | $1A'$ | 0.42 | 3.51 | 0.41 | 3.38 | 0.47 | 3.51 | |
| $(CO)_2Au_5^-$ | 2-a | $C_s$ | 1A | 0.00 | 3.53 | 0.00 | 3.41 | 0.00 | 3.34 | 3.41(3) |
| | 2-b | $C_{2v}$ | $1A'$ | 0.07 | 2.91 | 0.06 | 2.74 | 0.25 | 2.68 | |
| | 2-c | $C_{2v}$ | $1A_1$ | 0.16 | 2.85 | 0.13 | 2.72 | 0.27 | 2.87 | |
| | 2-d | $C_s$ | 1A | 0.18 | 3.36 | 0.16 | 3.25 | 0.21 | 3.39 | |
| | 2-e | $C_{2v}$ | 1A | 0.19 | 3.35 | 0.12 | 3.09 | 0.38 | 3.26 | |
| $(CO)_3Au_5^-$ | 3-a | $C_s$ | 1A | 0.00 | 3.18 | 0.11 | 2.99 | 0.24 | 2.95 | 2.91(3) |
| | 3-b | $C_s$ | 1A | 0.08 | 3.10 | 0.00 | 2.84 | 0.11 | 2.72 | |
| | 3-c | $C_1$ | 1A | 0.12 | 3.29 | 0.23 | 3.08 | 0.34 | 3.02 | |
| | 3-d | $C_s$ | 1A | 0.20 | 3.70 | 0.24 | 3.26 | 0.00 | 3.25 | |
| | 3-e | $C_s$ | 1A | 0.24 | 3.09 | 0.23 | 3.01 | 0.32 | 2.97 | |
| $(CO)_4Au_5^-$ | 4-a | $C_{2v}$ | 1A | 0.00 | 3.29 | 0.00 | 3.02 | 0.08 | 2.87 | |
| | 4-b | $C_s$ | 1A | 0.05 | 2.82 | 0.035 | 2.69 | 0.04 | 2.60 | 2.58(3) |
| | 4-c | $C_{2v}$ | $1A_1$ | 0.11 | 2.58 | 0.21 | 2.47 | 0.00 | 2.22 | |
| | 4-d | $C_s$ | 1A | 0.17 | 2.81 | 0.17 | 2.55 | | | |
| | 4-e | $C_s$ | 1A | 0.30 | 3.20 | 0.38 | 3.11 | 0.10 | 3.11 | |
| $(CO)_5Au_5^-$ | 5-a | $C_1$ | 1A | 0.00 | 2.72 | 0.016 | 2.60 | 0.00 | 2.96 | 2.60(3) |
| | 5-b | $C_{2v}$ | 1A | 0.02 | 2.78 | 0.00 | 2.66 | 0.15 | 2.99 | |
| | 5-c | $C_1$ | 1A | 0.65 | 2.96 | 0.79 | 2.84 | | | |
| | 5-d | $C_s$ | 1A | 0.84 | 3.07 | 0.95 | 2.97 | | | |
| | 5-e | $C_1$ | 1A | 0.86 | 3.14 | 0.94 | 2.87 | 0.38 | 2.64 | |

## Geometries of $(CO)_nAu_5^-$ (***n*** =1–5) complexes

To find the CO adsorption sites on the gold pentamer, we search a variety of isomers for $(CO)_nAu_5^-$ (n =1–5). Optimized most stable and selected low-lying isomers for $(CO)_nAu_5^-$ at PBE level are presented in Fig. 1. Meanwhile, the relative energies (RE) and the first VDEs at difference XC functionals are shown in Table 1. Upon chemisorption of a singe CO, the experimental spectrum of $(CO)Au_5^-$ induced a huge blue-shift of 0.85 eV, suggesting that the structure of $(CO)Au_5^-$ cluster may be significantly different from that of the parent $Au_5^-$. The most stable isomer 1-a can be formed by CO occupying an apex site of the V-shaped $Au_5^-$ isomer. The CO chemisorption leads to a slight structure distortion in the $Au_5^-$ motif: the distance of the two terminal Au atoms is slightly elongated. The terminal site adsorption (1-b) is less stable by 0.27 eV. The CO adsorption on the two-coordination gold atom of the optimal trapezoidal isomer is found to be higher in energy by 0.31 eV (1-c). While upon the four-coordinated gold site, the parent trapezoidal $Au_5^-$ framework transforms to the V-shaped one. In other words, the CO chemisorption induces the structure transformation between the isomers 0-a and 0-b. For the $(CO)Au_5^-$, all three different XC functionals prefer the $C_{2V}$ isomer 1-a. In addition, the calculated VDE is 3.73 eV, and is somewhat underestimated compared to experimental measurement (4.02 eV). The X-A gap derived from TD-DFT approach is 0.67 eV, and in prefect agreement with the experimental result ~0.70 eV (in Fig. 2) [25]. Moreover, upon the first CO chemisorption, the significant structural change of $Au_5$ substrate in $(CO)Au_5^-$ may be the reason of the huge blue-shift.

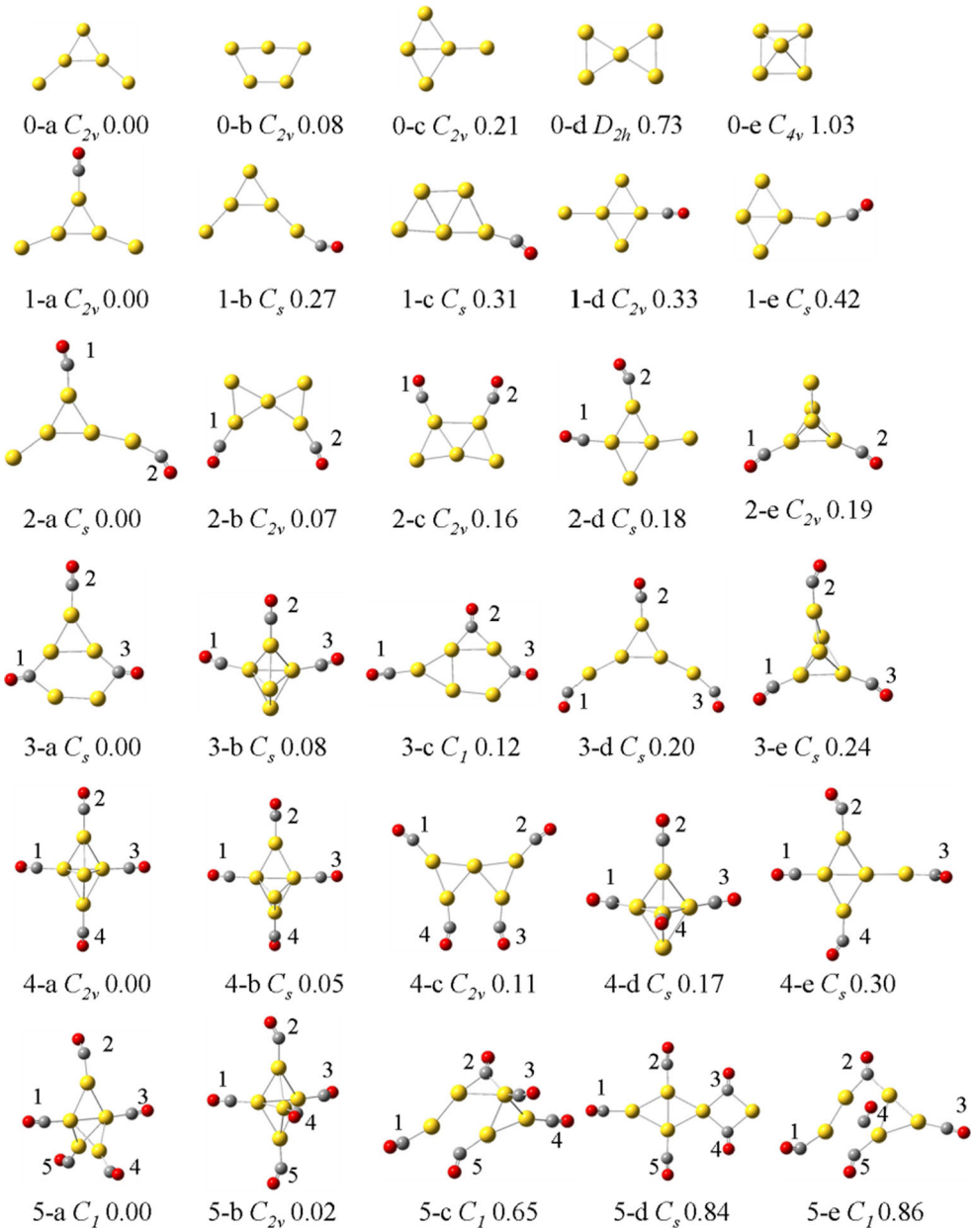


**Fig. 1** The lowest-energy and low-lying structures of $(CO)_nAu_5^-$ ($n$ =0–5). The corresponding point group symmetries along with relative stabilities are presented at the PBE level

Upon two CO molecules adsorption, the peak X of the spectrum of $(CO)_2Au_5^-$ (experimental VDE: 3.41 eV) is red-shifted appreciably compared to that of $(CO)Au_5^-$ [25]. The most stable structure of $(CO)_2Au_5^-$ is formed by adsorbing a CO molecule on the terminal gold site of the isomer 1-a. The second low-lying isomer 2-b is almost degenerate with energy difference of 0.07 eV, and can be generated when a CO molecule upon the two-coordination gold atom of the isomer 1-c, inducing the Au-Au bond breaking. The $Au_5$ motif in the structure 2-b is similar to the isomer 0-d. The isomer 2-c reported in previous literature is found to be less stable in energy by 0.16 eV [36]. The 3D side capped tetrahedral structure with two CO respectively adsorbing on the apex three-coordination gold atoms is $C_{2V}$ symmetry and 0.19 eV higher in energy. For the most stable isomer 2-a, the calculated VDEs are 3.53, 3.41, and 3.34 eV at PBE, TPSS, and B3LYP levels, respectively. The X-A gap is reported to be 0.93 eV. The results agree well with experiment (VDE: 3.41 eV, X-A gap: 1.11 eV), indicating that the isomer 2-a is the superlative candidate.

Upon the adsorption of three CO molecules, the first PES band seemed to show a splitting. The difference of the experiment spectrum indicates emergence of isomers with new structures. Indeed, the isomers 3-a, 3-b, and 3-c of $(CO)_3Au_5^-$ possess different structures compared to those of $(CO)Au_5^-$ or $(CO)_2Au_5^-$. Isomers 3-a and 3-c have similar $Au_5$ skeletons, which is distorted from the isomer 0-a upon CO adsorption. Surprisingly, not all three corner sites are

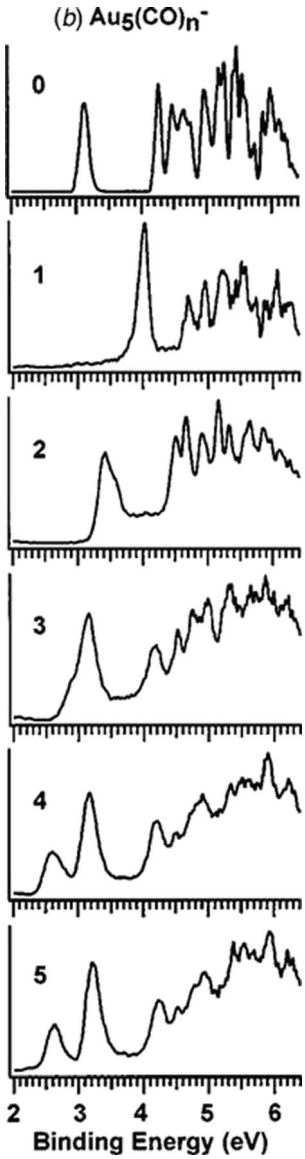


**Fig. 2** Photoelectron spectra of the $(CO)_nAu_5^-$ ($n$ =0–5) clusters are taken from ref. [25]

bonded with CO ligands in isomers 3-a and 3-c. Instead, a two bridged site is observed in both isomers. To our knowledge, that a bridged site is preferred over a sharp corner site by a legand has not been reported in gold clusters even though CO is largely known to prefer the corner (apex) sites [22–24, 27]. The second low-lying isomer 3-b is a 3D structure formed by a trigonal bipyramidal framework with three CO occupied on the corner site, and less stable than isomer 3-a in 0.08 eV at PBE level, but more stable in 0.11 eV at TPSS level. The isomer 3-d is generated when a CO molecule adsorbs on the terminal gold atom of the most stable isomer $(CO)_2Au_5^-$. The total energy of isomer 3-d is 0.20 eV lower than that of 3-a at PBE level, but isomer 3-d is predicted to be the lowest energy isomer at B3LYP level. According to the second criteria, the calculated VDEs of isomer 3-a are 3.18, 2.99, and 2.95 eV at PBE, TPSS, and B3LYP level, respectively, and consistent with experimental data (2.91 eV). So, the isomer 3-a is ground state.

Subsequent CO adsorption each produces red-shift up to n =4, beyond which both the electron binding energy and spectral pattern change a little. Starting at $(CO)_4Au_5^-$, the first PES band can be seen more clearly splitting. The lowest energy isomer 4-a at PBE and TPSS levels, can be obtained by a CO molecule chemisorbing on the apex site of the isomer 3-b. The 3D isomer 4-b are calculated to be degenerate with isomer 4-a (RE =0.05 eV at PBE level; RE =0.035 eV level at TPSS). The planar structure 4-c is predicted to be the most stable isomer at B3LYP level, and can be formed by four CO molecules adsorbing on the available four low coordination sites in the trapezoidal $Au_5$ substrate. The VDE of isomer 4-a is calculated to be 3.29 eV. It is far away from the first VDE (2.58 eV), but closed to the splitted band (~3.22 eV) [25]. The VDEs of isomers 4-b and 4-c are 2.82 and 2.58 eV, and in reasonable agreement with the first band (2.58 eV). Thus it is concluded that all three isomers 4-a, 4-b, and 4-c are likely coexisting in the cluster beam.

The lowest energy isomer 5-a of $(CO)_5Au_5^-$ at PBE level is also a 3D structure in which the $Au_5$ framework is rearranged to a side capped tetrahedral structure. The isomer 5-b is preferred at TPSS level, in which the $Au_5$ substrate has trigonal bipyramidal geometry. In both $Au_5$ frameworks, all five Au atoms become apex sites to accommodate the five CO molecules. The calculated VDEs of both isomer 5-a and 5-b are 2.72 and 2.78 eV at PBE level, and overestimated with experimental measurement (2.60 eV). The PES spectrum of $(CO)_5Au_5^-$ has very little change compared to that of $(CO)_4Au_5^-$. Clearly, PES is quite sensitive to the adsorbate-clusters interactions and provides spectroscopic means to distinguish between chemisorption versus physisorption. The structural transformation of $Au_5$ skeleton is to create more apex sites to accommodate the additional CO molecules. When upon the fifth CO molecule adsorption, both the electron binding energies and spectral pattern change little between n =4 and 5. For isomer 5-a and 5-b, the five CO molecules adsorb on the apex sites, and calculated VDEs are slightly overestimated, indicating that the fifth CO molecule adsorption regime is different from the experimental predicted physisorption regime.

To further understand the CO molecule adsorption regime, the distances of Au-C ($R_{Au-C}$) and C-O ($R_{C-O}$) bonding are obtained and presented in Table 2, at the PBE level. It is found that $R_{Au-C}$ is shorter than 2 Å at the corner (apex) sites of $(CO)_nAu_5^-$ ($n$ =1–4) and somewhat longer than 2 Å at that in $(CO)_5Au_5^-$, indicating that the fifth CO adsorption in $(CO)_nAu_5^-$ cluster is weaker than that in $(CO)_nAu_5^-$ ($n$ =1–4). For bridged site CO, the $R_{Au-C}$ is relatively large, and all beyond 2 Å. $R_{C-O}$ is in the range from 1.153 to 1.164 Å at the corner (apex) sites chemisorption, and somewhat larger than that of pure CO molecule (1.136 Å). For the bridged site, $R_{C-O}$ is comparable large and beyond

**Table 2** HOMO-LUMO gap Δ (eV), the distances of Au-C and C-O bonds (Å), CO vibration frequencies ($cm^{-1}$), and binding energies BE (eV) for the $(CO)_nAu_5^-$ (n =0–5) clusters at PBE level

| Geo. | Δ | $R_{Au-C}$ | $R_{C-O}$ | Freq. | BE(n) | BE(CO) |
|---|---|---|---|---|---|---|
| 1-a | 1.572 | 1.915 | 1.153 | 2027 | 1.15 | 1.15 |
| 1-b | 1.786 | 1.962 | 1.157 | 1977 | 0.88 | 0.88 |
| 1-c | 1.159 | 1.955 | 1.160 | 1958 | 0.84 | 0.84 |
| 1-d | 1.606 | 1.934 | 1.154 | 2012 | 0.82 | 0.82 |
| 1-e | 1.736 | 1.954 | 1.158 | 1973 | 0.74 | 0.74 |
| 2-a | 1.493 | 1.927, 1.984 | 1.155, 1.159 | 1956, 2007 | 1.00 | 0.84 |
| 2-b | 1.294 | 1.191, 1.191 | 1.160, 1.160 | 1986, 1969 | 0.96 | 0.77 |
| 2-c | 1.124 | 1.931, 1.931 | 1.159, 1.159 | 1986, 1966 | 0.92 | 0.67 |
| 2-d | 1.423 | 1.938, 1.956 | 1.156, 1.158 | 1966, 1996 | 0.91 | 0.66 |
| 2-e | 1.593 | 1.925, 1.925 | 1.160, 1.160 | 1964, 1979 | 0.90 | 0.65 |
| 3-a | 1.341 | 2.071(2.118), 1.933, 2.051(2.149) | 1.178, 1.157, 1.178 | 1827, 1835, 1991 | 0.99 | 0.97 |
| 3-b | 1.406 | 1.923, 1.923, 1.933 | 1.161, 1.159, 1.161 | 1960, 1964, 1987 | 0.96 | 0.89 |
| 3-c | 1.102 | 1.933, 2.045(2.130), 2.078(2.124) | 1.156, 1.182, 1.181 | 1810, 1834, 1993 | 0.95 | 0.85 |
| 3-d | 1.482 | 1.998, 1.950, 1.995 | 1.161, 1.156, 1.161 | 1938, 1946, 1985 | 0.92 | 0.77 |
| 3-e | 1.456 | 1.932, 1.949, 1.934 | 1.161, 1.161, 1.161 | 1943, 1953, 1972 | 0.91 | 0.73 |
| 4-a | 1.503 | 1.919, 1.970, 1.919, 1.970 | 1.162, 1.162, 1.162, 1.162 | 1938, 1940, 1956, 1982 | 0.93 | 0.77 |
| 4-b | 1.075 | 1.923, 1.988, 1.923, 1.953 | 1.160, 1.161, 1.160, 1.163 | 1934, 1941, 1967, 1990 | 0.92 | 0.72 |
| 4-c | 0.784 | 1.948, 1.948, 1.954, 1.954 | 1.161, 1.161, 1.161, 1.161 | 1937, 1948, 1956, 1991 | 0.91 | 0.67 |
| 4-d | 0.957 | 1.985, 1.930, 1.984, 1.903 | 1.164, 1.159, 1.164, 1.164 | 1909, 1919, 1954, 1984 | 0.89 | 0.60 |
| 4-e | 1.392 | 1.958, 1.990, 1.999, 1.990 | 1.158, 1.162, 1.161, 1.162 | 1927, 1929, 1944, 1978 | 0.86 | 0.48 |
| 5-a | 0.958 | 1.919, 1.979, 1.919, 1.997, 2.015 | 1.161, 1.159, 1.161, 1.164, 1.165 | 1902, 1919, 1951, 1958, 1987 | 0.87 | 0.62 |
| 5-b | 1.044 | 1.900, 1.975, 1.986, 1.986, 1.975 | 1.165, 1.161, 1.164, 1.164, 1.161 | 1908, 1914, 1938, 1939, 1972 | 0.86 | 0.60 |
| 5-c | 1.060 | 2.051, 2.105(2.116), 1.973, 1.938, 2.052 | 1.162, 1.181, 1.161, 1.157, 1.173 | 1811, 1849, 1920, 1945, 1988 | 0.74 | −0.02 |
| 5-d | 0.955 | 2.019, 1.942, 2.237(2.263), 2.237(2.263), 1.942 | 1.162, 1.155, 1.170, 1.170, 1.155 | 1855, 1886, 1920, 1993, 2014 | 0.70 | −0.22 |
| 5-e | 1.048 | 2.039, 2.115(2.096), 1.935, 2.826, 2.030 | 1.159, 1.178, 1.158, 1.143, 1.170 | 1831, 1873, 1945, 1987, 2055 | 0.69 | −0.24 |

1.170 Å. It is worthy pointing out that $R_{Au-C}$ and $R_{C-O}$ are elongated in the bridged site chemisorption, indicating that the strength of Au-C and C-O bonding in the bridged CO is weakened compared to that in the corner (apex) CO. For $(CO)_5Au_5^-$, the elongated $R_{Au-C}$ in the apex site CO suggests the weak Au-C bonding.

For $(CO)_nAu_5^-$ ($n$ =0–5) complexes, the different XC functionals (PBE, TPSS, and B3LYP) have obtained the consensus results at the lowest energy isomers when $n$ =0–2, and the predicted VDEs have little disparity. When n ≥3, the most stable isomers are different according to different XC functionals calculations. It is found that the B3LYP functional is not reliable for the $(CO)_nAu_5^-$ ($n$ =0–5) complexes. The calculated VDEs of the same structures at B3LYP level have a fluctuant tendency compared to those at PBE level. The TPSS results are always lower than PBE ones, and the trends predicted at PBE and TPSS levels are in agreement with the experimental results. The apex sites in parent $Au_5^-$ cluster are not always the most preferred sites for the CO adsorption. Even with chemisorption of a single CO, a major structural change occurs at parent $Au_5^-$ cluster.

## CO adsorption-induced 2D to 3D structure transformation

For CO adsorption upon $Au_7^-$ cluster, it is found that CO binding can induce the unique 2D–3D–2D structural change. Thus one may ask how the structural change occurs in $Au_5^-$ framework upon CO adsorption. In Fig. 3, we compare the relative stabilization energy of the most stable 2D and 3D isomers of complexes with a different number of CO

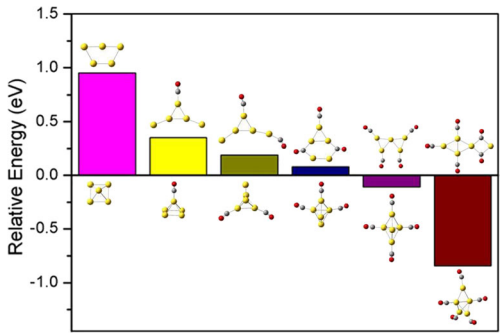


**Fig. 3** Relative stabilization energies at PBE level for the most stable 2D and 3D isomers of $Au_5^-$ anion cluster with different number of CO molecules adsorbed

molecules at PBE level. The bare $Au_5^-$ cluster has a planar structure with stabilization energy of 0.95 eV compared to the 3D geometry structure. Upon the first CO adsorption, a large structural change occurs in $Au_5$ framework and induces a large blue-shift in the experimental spectrum. Meanwhile, the relative energy between 2D and 3D isomers decreases to 0.35 eV. The 3D $Au_5$ motif in the $(CO)_2Au_5^-$ is totally different from the 3D $Au_5^-$ structure. Thus the second CO adsorption induces a major structural change to the 3D $Au_5$ substrate. In addition, the relative energy further decreases to 0.19 eV. Upon the third CO molecule adsorption, the bridged site is preferred over the apex site in the 2D $(CO)_3Au_5^-$. Moreover, the 2D and 3D structures are almost degenerate, and the 2D structure is more stable with stabilization energy of 0.08 eV. It turns out that the CO adsorption tends to stabilize the 3D structure relative to the planar one. Indeed, upon the forth CO adsorption, the gold cluster no longer retains its planar structure, leading to the 2D-3D structural transformation. The 3D structure of $(CO)_4Au_5^-$ is 0.11 eV lower in energy than the planar structure. Upon the fifth CO molecule adsorption, the relative energy between the 2D and 3D structures increases to 0.84 eV. This significant 2D-3D structural transition suggests that the anion gold pentamer is flexible and its structures are strongly dependent on CO adsorption and coverage. Structural flexibility has been suggested to be important during catalytic reactions.

## IR spectrum

The frequencies of the adsorbate in the most stable $(CO)_nAu_5^-$ ($n$ =1–5) clusters are calculated at PBE level, and listed in Table 2. Meanwhile, the IR spectra are presented in Fig. 4. Vibrational frequency analysis not only indicates if an optimized structure is a local minimum on the potential energy surface but also performs the determination of the corresponding IR spectrum. Therefore, it can provide a spectroscopic fingerprint to distinguish between different species and different clusters. The IR spectrum for the trapezoidal $Au_5^-$ has four dominant peaks. The most intense peak locates at 172 $cm^{-1}$. The spectrum for V-shaped $Au_5^-$ is quite simple with only two peaks and the highest intensity peak locates at 166 $cm^{-1}$. A great difference in IR spectrum between those two isomers can provide a method to distinguish the true global minimum. Upon the CO adsorption, the most intense peaks in these spectra are generally associated with the vibrational motions of CO molecules, and those of $Au_5$ substrate are found in the far-infrared region (100–400 $cm^{-1}$). With regard to $(CO)Au_5^-$, one well-marked peak locates at 2027 $cm^{-1}$, and is substantially red-shift compared to bare CO (2134 $cm^{-1}$). Upon the second CO molecule adsorption, there are two visible peaks in the IR spectrum. The highest intensity peak locates at 1956 $cm^{-1}$ and is slightly red-shifted. As to $(CO)_3Au_5^-$, the CO frequency $\nu$(CO) in the bridged site adsorption are 1827 and 1835 $cm^{-1}$ considerably red-shifted. The bridge CO on $Au_5$ has been observed as a feature at 1853 $cm^{-1}$ from the low-temperature matrix IR spectra measurements [36]. Our calculated $\nu$(CO) in the bridged site is consistent with the experimental measurements. Due to vibrational minority in the bridged site CO molecules, IR spectrum has two obvious peaks. For $(CO)_4Au_5^-$, the most intense peak locates at 1940 $cm^{-1}$, and is blue-shifted compared to the bridged adsorption $(CO)_3Au_5^-$. The largest $\nu$(CO) of 1982 $cm^{-1}$ is in agreement with the experimental observation (2003 $cm^{-1}$) [36]. The IR spectrum of $(CO)_5Au_5^-$ has three perceptible peaks and two inconspicuous peaks. It is worth pointing out that vibrational mode in the corner (apex) site CO is different from that in the bridged site CO. Chemical bonding in transition metal carbonyl complexes (M-CO) comprise M←CO σ donation or M→CO π back-donation, CO is both σ donor and π acceptor ligand [37]. The CO stretching frequency is a useful indicator of the magnitude of σ- and π-bonding in the metal carbonyl. In classical M-CO transition metal complexes, strong M→CO π back-donation weakens the CO bond, resulting in a red-shift in the CO stretching frequency. However, strong σ-donation or weak π back-donation can lead to stronger CO bonding and an increased CO stretching frequency in nonclassical M-CO complexes. Surface studies show that CO stretching frequency in Au(0)-CO species is at ~2110 $cm^{-1}$ [38], where the red-shift relative to free CO molecule is small. Our current calculation of CO stretching frequencies are almost equal or less than 2000 $cm^{-1}$ in $(CO)_nAu_5^-$ (n =1–5), and all are red-shift.

## Electronic properties

Aiming to probing into the localization of the charge in CO molecules of $(CO)_nAu_5^-$ clusters and reliable charge-transfer information, the natural population analysis (NPA) have been calculated at PBE level and summarized in Table 3. The serial number of CO molecules is deasil labeled in Fig. 1. It clearly shows that the natural charges of C atoms are positive and those of O atoms are negative. The natural charges of CO molecules are various in different species, and those on the same symmetry site in the same isomer are the same. The sum charge on CO molecule is positive, indicating that the extra electron is shared by parent $Au_5$ cluster. It means that electron density flows from CO to parent cluster, and the CO donation is probably the dominant mechanism. While the natural charge on CO is negative, indicating the electron density flows from parent cluster to CO for CO back-donation regime. For the multi-CO adsorption upon $Au_5^-$ cluster, positive and negative charge distribution is simultaneous, indicating that the donation and back-donation mechanisms play a cooperative role in the multi-CO adsorption on the anion gold pentamer.

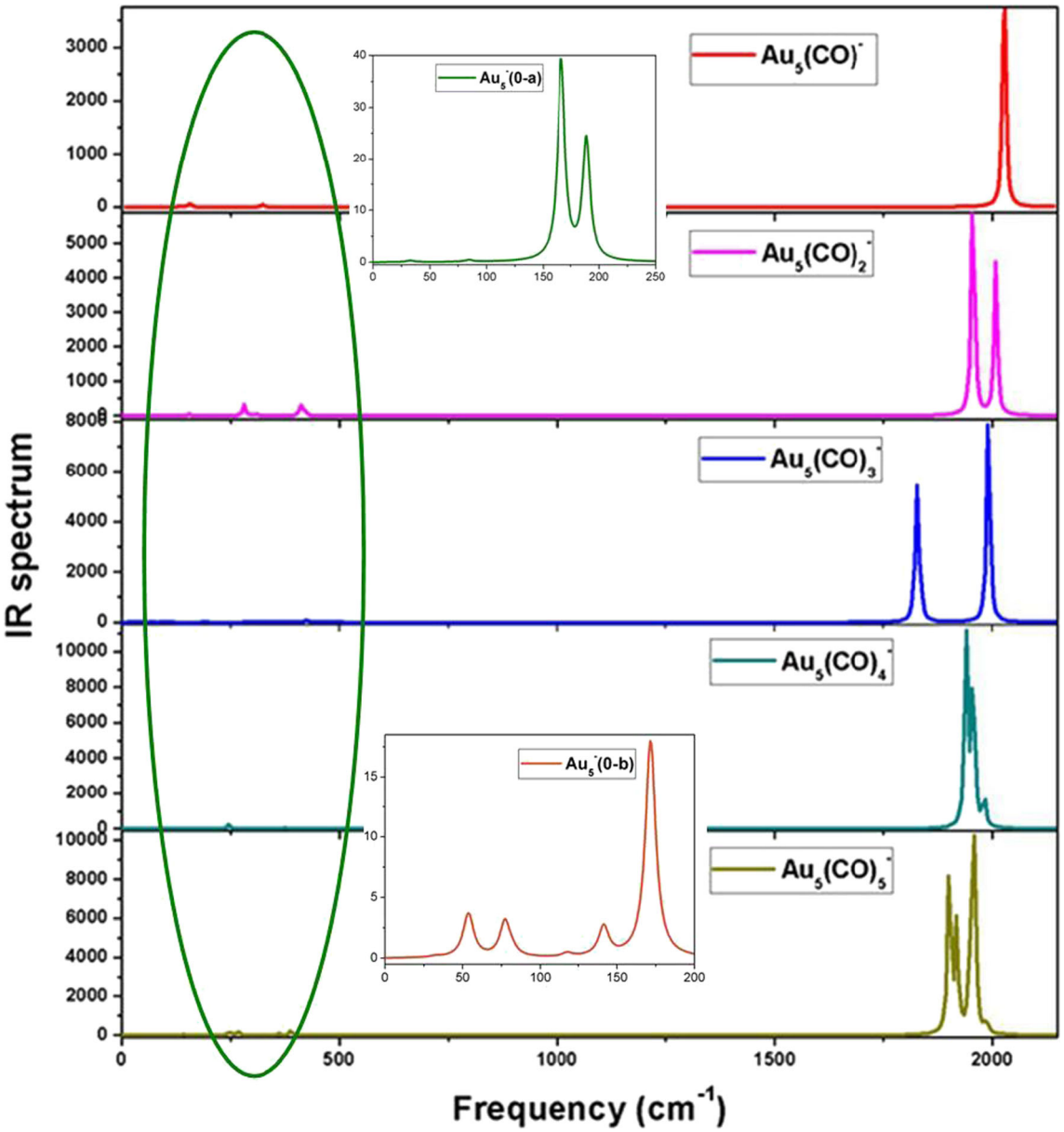


**Fig. 4** IR spectra of the $(CO)_nAu_5^-$ ($n$ =0–5) clusters at PBE level

Binding energies

Based on the PBE level, relative stabilities of the clusters $(CO)_nAu_5^-$ (n =1–5) are investigated on the basis of two forms of binding energies (BEs): (1) BE(n)={nE(CO)+E($Au_5^-$)-E($(CO)_nAu_5^-$)}/n, and (2) BE(CO)=E(CO)+E($(CO)_{n-1}Au_5^-$) – E($(CO)_nAu_5^-$). The E(CO), E($Au_5^-$), and E($(CO)_{n-1}Au_5^-$) are the total energies of CO molecule and the lowest-energy $Au_5^-$ and $(CO)_{n-1}Au_5^-$ isomers. The E($(CO)_nAu_5^-$) are the total energies of the lowest energy and low-lying isomers of $(CO)_nAu_5^-$ clusters. The BE(n) measures the average interaction between parent gold pentamer and CO molecules, and BE(CO) refers to the interaction between the complex and the subsequently adsorbed CO. The resulting calculated binding energy values are also included in Table 2. As seen in Table 2, the average binding energies BE(n) decrease gradually with the relative energies, and those of the lowest energy isomers decrease gradually with n. As to BE(CO), it is found that the binding energy of the lowest energy isomer decreases with cluster size except n =3, indicating that the interaction between the CO molecule and parent cluster weakens upon subsequent CO adsorption. The BE of the lowest energy structure of one complex is totally higher than that of low-lying structure, suggesting that the lowest energy is more stable than the low-lying structure. It is worth pointing out that the BE(CO) of the bridged CO adsorption $(CO)_3Au_5^-$ (3-a) is anomalously increasing compared to $(CO)_2Au_5^-$ (2-a). The cooperation of two relatively weak Au-C bonds in

**Table 3** Natural charge populations of C and O atoms for the $(CO)_nAu_5^-$ (n =1–5) clusters at PBE level. The numbers are labeled in Fig. 1

| Geo. | C-1 | O-1 | C-2 | O-2 | C-3 | O-3 | C-4 | O-4 | C-5 | O-5 |
|---|---|---|---|---|---|---|---|---|---|---|
| 1-a | 0.438 | −0.418 | | | | | | | | |
| 1-b | 0.387 | −0.435 | | | | | | | | |
| 1-c | 0.381 | −0.448 | | | | | | | | |
| 1-d | 0.466 | −0.430 | | | | | | | | |
| 1-e | 0.409 | −0.437 | | | | | | | | |
| 2-a | 0.367 | −0.443 | 0.425 | −0.422 | | | | | | |
| 2-b | 0.398 | −0.443 | 0.399 | −0.448 | | | | | | |
| 2-c | 0.415 | −0.445 | 0.415 | −0.445 | | | | | | |
| 2-d | 0.388 | −0.439 | 0.457 | −0.441 | | | | | | |
| 2-e | 0.484 | −0.405 | 0.484 | −0.405 | | | | | | |
| 3-a | 0.205 | −0.436 | 0.219 | −0.423 | 0.483 | −0.395 | | | | |
| 3-b | 0.443 | −0.423 | 0.471 | −0.427 | 0.472 | −0.427 | | | | |
| 3-c | 0.175 | −0.470 | 0.186 | −0.453 | 0.407 | −0.441 | | | | |
| 3-d | 0.343 | −0.455 | 0.346 | −0.454 | 0.407 | −0.435 | | | | |
| 3-e | 0.394 | −0.433 | 0.430 | −0.437 | 0.432 | −0.436 | | | | |
| 4-a | 0.382 | −0.453 | 0.382 | −0.453 | 0.452 | −0.456 | 0.452 | −0.456 | | |
| 4-b | 0.383 | −0.460 | 0.383 | −0.460 | 0.389 | −0.448 | 0.389 | −0.448 | | |
| 4-c | 0.357 | −0.453 | 0.371 | −0.459 | 0.464 | −0.454 | 0.464 | −0.454 | | |
| 4-d | 0.385 | −0.460 | 0.389 | −0.458 | 0.410 | −0.438 | 0.449 | −0.461 | | |
| 4-e | 0.355 | −0.460 | 0.366 | −0.450 | 0.367 | −0.450 | 0.459 | −0.449 | | |
| 5-a | 0.350 | 0.456 | 0.360 | −0.450 | 0.391 | −0.440 | 0.469 | −0.448 | 0.473 | −0.447 |
| 5-b | 0.367 | −0.472 | 0.367 | −0.472 | 0.369 | −0.461 | 0.433 | −0.450 | 0.408 | −0.437 |
| 5-c | 0.215 | −0.465 | 0.259 | −0.456 | 0.358 | −0.461 | 0.433 | −0.450 | 0.408 | 0.437 |
| 5-d | 0.270 | −0.451 | 0.270 | −0.451 | 0.377 | −0.422 | 0.472 | −0.402 | 0.472 | 0.402 |
| 5-e | 0.206 | −0.457 | −0.298 | −0.452 | 0.382 | −0.449 | 0.415 | −0.439 | 0.492 | −0.467 |

the bridged CO is stronger than the single strong Au-C bond in the corner CO. For the $(CO)_5Au_5^-$ complexes, BE of isomers 5-a and 5-b are 0.62 and 0.60 eV, and those of isomers 5-c, 5-d, and 5-e are -0.02, -0.22, and -0.24 eV, respectively. Why dose the BE change significantly? We further check the structure of those isomers. It is found that the gold substrates in isomers 5-a and 5-b have five available apex sites to accommodate the five CO molecules, but two CO molecules that shared one Au atom emerged in isomers 5-c, 5-d, and 5-e. The calculated BE of the isomers 5-a and 5-b are relatively large, indicating that the fifth CO molecule adsorption on these isomers is not weak physisorption regime. The BE of isomers 5-c, 5-d, and 5-e are all less than zero, implying that the interaction between the fifth CO molecule and substrate is comparatively feeble in physisorption regime.

For the lowest energy isomers of $(CO)_nAu_5^-$ clusters, we further study the fragmentation energy by dropping CO

**Table 4** Fragmentation energies $E_F$ (eV) of the lowest-energy $(CO)_nAu_5^-$ (n =1–5) clusters at PBE level for various channels by dropping a different number of CO molecules

| Cluster | $E_F$ | | | | |
|---|---|---|---|---|---|
| | 1 | 2 | 3 | 4 | 5 |
| $(CO)Au_5^-$ | 1.15 | | | | |
| $(CO)_2Au_5^-$ | 0.84 | 1.99 | | | |
| $(CO)_3Au_5^-$ | 0.97 | 1.81 | 2.96 | | |
| $(CO)_4Au_5^-$ | 0.77 | 1.74 | 2.58 | 3.74 | |
| $(CO)_5Au_5^-$ | 0.62 | 1.40 | 2.36 | 3.20 | 4.36 |

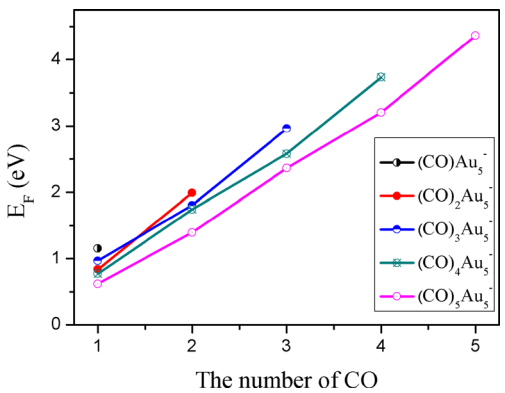


**Fig. 5** Fragmentation energies of $(CO)_nAu_5^-$ (*n* =1–5) clusters at PBE level for dropping a different number of CO molecules

molecules one by one according to $E_F((CO)_nAu_5^-)=mE(CO)+E((CO)_{n-m}Au_5^-) - E((CO)_nAu_5^-)$ $(1\leq m\leq n \leq 5)$. Meanwhile, the results are listed in Table 4. The fragmentation energy as the number of CO molecules lost is presented in the Fig. 5. Clearly, for one specie, the fragmentation energy increases by singly dissociating the CO molecule. For the $(CO)_3Au_5^-$ complex, the second CO molecule dissociation is easier than the first and third CO molecules, implying that the second CO molecule may be on the corner site, and the first and third CO are on the bridged site. After losing two molecules, the Au-C bond rupture energies increase disproportionally, indicating that further dissociating CO molecules becomes easier. As for the $(CO)_5Au_5^-$ complex, it is easy to drop the first two molecules, and relatively difficult to further dissociate.

## Conclusions

In summary, we have investigated the geometry properties, structural transition, chemisorption, and physisorption regime of the gold pentamer upon multi-CO adsorption with density functional calculations. All results are summarized as follows:

1) Even with chemisorption of a single CO, a major structural change occurs in $Au_5^-$. The apex sites in the parent $Au_5^-$ cluster are not always the most perfect sites for the chemisorption, and two bridged adsorption CO molecules are observed in the $(CO)_3Au_5^-$ cluster.
2) The 2D-3D structural transformation occurs at n =4, suggesting that the $Au_5^-$ cluster is flexible and its structures are strongly dependent on CO chemisorption and coverage. Structure flexibility has been suggested to be important during catalytic reactions. The $Au_5^-$ cluster may be an example to study structural flexibility in a small 2D gold cluster and how their structures can adapt to different reaction conditions to enable catalytic reaction.
3) The IR spectra are discussed by vibrational frequency analysis. It is found that the CO stretching frequency in $(CO)_nAu_5^-$ complexes are red-shifted compared to free CO molecule.
4) Based on the binding energies (BE) and fragmentation energies calculations, the cooperation of two bridged CO is stronger than single corner adsorption. Furthermore, BE of the fifth apex site adsorption, together with the vertical electron detachment energy (VDE), and Au-C bind distance analysis for the $(CO)_5Au_5^-$ cluster, indicate that it is not a physisorption regime, and the chemisorption-saturated number is 5.

**Acknowledgments** This work was supported by the National Natural Science Foundation of China (No. 11274235 and No. 11104190) and the Doctoral Education Fund of Education Ministry of China (No. 20100181110086 and No. 20110181120112).

## References

1. Haruta M (1997) Catal Today 36:153–166
2. Bond GC, Thompson DT (1999) Rev Sci Eng 41:319–388
3. Haruta M (2003) Chem Rec 3:75–87
4. Nijhuis TA, Visser T, Weckhuysen BM (2005) J Phys Chem B 109: 19309–19319
5. Sinha AK, Seelan S, Tsubota S, Haruta M (2004) Top Catal 29: 95–102
6. McEwan L, Julius M, Roberts S, Fletcher JCQ (2010) Gold Bull 43: 298–306
7. Tsunoyama H, Sakurai H, Ichikuni N, Negishi Y, Tsukuda T (2004) Langmuir 20:11293–11296
8. Bond G (2009) Gold Bull 42:337–11296
9. Haruta M, Tsubota S, Kobayashi T, Kageyama H, Genet MJ, Delmon B (1993) J Catal 144:175–192
10. Valden M, Lai X, Goodman DW (1998) Science 281:1647–1650
11. Yoon B, Hakkinen H, Landman U, Worz AS, Antonietti JM, Abbet S, Judai K, Heiz U (2005) Science 307:403–407
12. Sanchez A, Abbet S, Heiz U, Schneider WD, Hakkinen H, Barnett RN, Landman U (1999) J Phys Chem A 103:9573–9578
13. Chen MS, Goodman DW (2004) Science 306:252–255
14. Lemire C, Meyer R, Shaikhutdinov S, Freund HJ (2004) Angew Chem Int Ed 43:118–121
15. Lopez N, Janssens TVW, Clausen BS, Xu Y, Mavrikakis M, Bligaard T, Norskov JK (2004) J Catal 223:232–235
16. Yuan DW, Zeng Z (2004) J Chem Phys 120:6574–6584
17. Fernández EM, Ordejón P, Balbás L (2005) Chem Phys Lett 408: 252–257
18. Neumaier M, Weigend F, Hampe O, Kappes MM (2005) J Chem Phys 122:104702
19. Hagen J, Socaciu LD, Elijazyfer M, Heiz U, Bernhardt TM, Wöste L (2002) Phys Chem Chem Phys 4:1707–1709
20. Socaciu LD, Hagen J, Bernhardt TM, Wöste L, Heiz U, Häkkinen H, Landman U (2003) J Am Chem Soc 125:10437–17505
21. Wallace WT, Whetten RL (2002) J Am Chem Soc 124:7499–7505
22. Zhai HJ, Kiran B, Dai B, Li J, Wang LS (2005) J Am Chem Soc 127: 12098–12106
23. Li J, Li X, Zhai HJ, Wang LS (2003) Science 299:864–867
24. Huang W, Bulusu S, Pal R, Zeng XC, Wang LS (2009) J Chem Phys 131:234305
25. Zhai HJ, Wang LS (2005) J Chem Phys 122:051101
26. Pal R, Huang W, Wang YL, Hu HS, Xiong XG, Bulusu S, Li J, Wang LS, Zeng XC (2011) J Phys Chem Lett 2:2288–2293
27. Zhai HJ, Pan LL, Dai B, Kiran B, Li J, Wang LS (2008) J Phys Chem A 112:11920–11928
28. Dolg M, Wedig U, Stoll H, Preuss H (1987) J Chem Phys 86:866
29. Schwerdtfeger P, Dolg M, Schwarz WHE, Bowmaker GA, Boyd PDW (1989) ibid, 91: 1762
30. Perdew JP, Burke K, Ernzerhof M (1996) Phys Rev Lett 77:3865–3868
31. Stephens PJ, Devlin FJ, Chabalowski CF, Frisch MJ (1994) J Phys Chem 98:11623–11627
32. Tao J, Perdew J, Staroverov V, Scuseria G (2003) Phys Rev Lett 91: 146401
33. Frisch MJ, Trucks GW, Schlegel HB, Scuseria GE, Robb MA, Cheeseman JR, Montgomery JJA, Vreven T, Kudin KN, Burant JC, Millam JM, Iyengar SS, Tomasi J, Barone V, Mennucci B, Cossi M, Scalmani G, Rega N, Petersson GA, Nakatsuji H, Hada M, Ehara M, Toyota K, Fukuda R, Hasegawa J, Ishida M, Nakajima T, Honda Y, Kitao O, Nakai H, Klene M, Li X, Knox JE, Hratchian HP, Cross JB, Bakken V, Adamo C, Jaramillo J, Gomperts R, Stratmann RE, Yazyev O, Austin AJ, Cammi R, Pomelli C, Ochterski J, Ayala PY, Morokuma K, Voth GA, Salvador P, Dannenberg JJ, Zakrzewski VG, Dapprich S, Daniels AD, Strain MC, Farkas O, Malick DK, Rabuck AD, Raghavachari K, Foresman

JB, Ortiz JV, Cui Q, Baboul AG, Clifford S, Cioslowski J, Stefanov BB, Liu G, Liashenko A, Piskorz P, Komaromi I, Martin RL, Fox DJ, Keith T, Al-Laham MA, Peng CY, Nanayakkara A, Challacombe M, Gill PMW, Johnson BG, Chen W, Wong MW, Gonzalez C, Pople JA (2004) Gaussian 03, revision E01. Gaussian Inc, Wallingford

34. Häkkinen H, Yoon B, Landman U, Li X, Zhai HJ, Wang LS (2003) J Phys Chem A 107:6168–6175
35. Häkkinen H, Moseler M, Landman U (2002) Phys Rev Lett 89: 033401
36. Fielicke A, Helden G, Meijer G, Simard B, Rayner D (2005) J Phys Chem B 109:23935–23940
37. Rack JJ, Strauss SH (1997) Catal Today 36:99–106
38. Meyer R, Lemire C, Shaikhutdinov SK, Freund HJ (2004) Gold Bull 37:72–124